Check for updates

How to cite: *Angew. Chem. Int. Ed.* **2021**, *60*, 17410–17414
International Edition: doi.org/10.1002/anie.202105718
German Edition: doi.org/10.1002/ange.202105718

Astrochemistry

Unveiling Five Naked Structures of Tartaric Acid

*Elena R. Alonso, Iker León, Lucie Kolesniková, Santiago Mata, and Jose Luis Alonso**

Abstract: *The unbiased, naked structures of tartaric acid, one of the most important organic compounds existing in nature and a candidate to be present in the interstellar medium, has been revealed in this work for the first time. Solid samples of its naturally occurring (R,R) enantiomer have been vaporized by laser ablation, expanded in a supersonic jet, and characterized by Fourier transform microwave spectroscopy. In the isolation conditions of the jet, we have discovered up to five different structures stabilized by intramolecular hydrogen-bond networks dominated by O–H···O=C and O–H···O motifs extended along the entire molecule. These five forms, two with an extended (trans) disposition of the carbon chain and three with a bent (gauche) disposition, can serve as a basis to represent the shape of tartaric acid. This work also reports the first set of spectroscopy data that can be used to detect tartaric acid in the interstellar medium.*

In 1848, Louis Pasteur unequivocally established the existence of molecular chirality with the tartaric acid (TA) molecule.[1] Previously, Biot discovered that (2R,3R) tartaric acid in aqueous solution was optically active and that racemic-tartaric acid was inactive.[2] It led Pasteur to study the morphology of several crystals of (2*R*,3*R*)-tartaric acid ((+)-TA) and of rare paratartaric acid (PTA) and their optical behavior in solution, establishing that the (2*R*,3*R*)- and (2*S*,3*S*)-tartrates are isometric and related one to another as non-superposable mirror images.[3] For all the above, TA is one of the most important organic compounds in stereochemistry history.[4] The naturally occurring form of tartaric acid corresponds to the stereoisomer (*R*,*R*) (see Figure 1), obtained from fermenting grape juice in the wine-making process.

TA is widely used in the pharmaceutical industry as an excipient and buffering agent and in foods and beverages as an acidulant, among other applications.[5] In the chemistry field, it is used as a chiral building block[6] to produce chiral ligands for metal-catalyzed reactions[7] and provide new organocatalysts.[8] In astrochemistry, TA is a potential molecule to be present in the interstellar medium (ISM). It has already been found in the Murchison meteorite.[9] Astrophy-

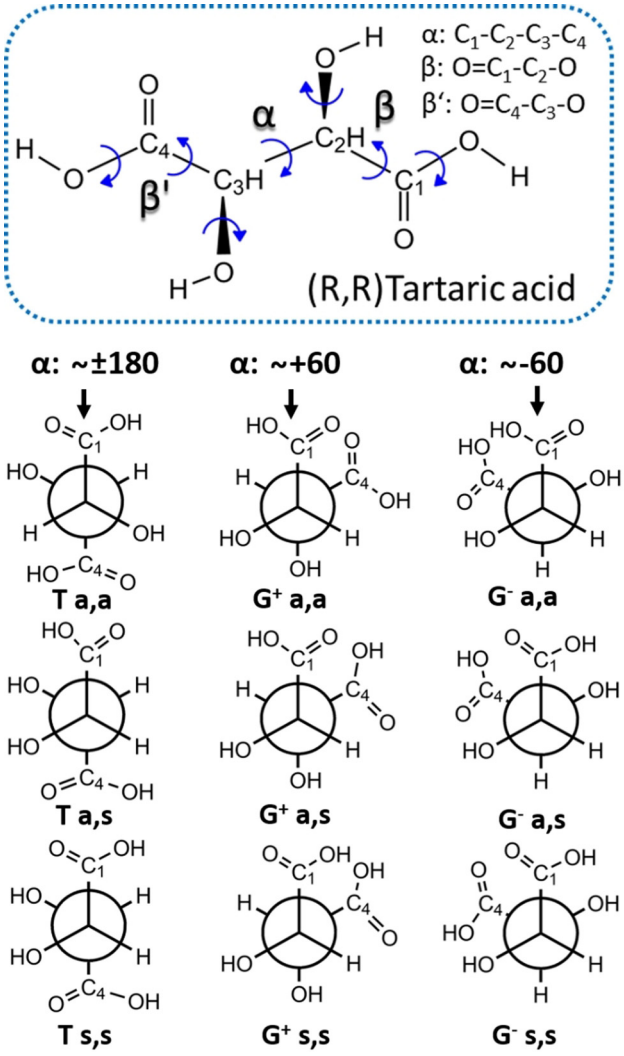

Figure 1. Configurational map of (*R*,*R*) tartaric acid based on Newman projections taking into account all its degrees of freedom.

[*] Dr. E. R. Alonso
Instituto Biofisika (UPV/EHU, CSIC)
University of the Basque Country
48940 Leioa (Spain)
and
Departamento de Química Física, Facultad de Ciencia y Tecnología, Universidad del País Vasco
Barrio Sarriena s/n, 48940 Leioa (Spain)
Dr. I. León, S. Mata, Prof. J. L. Alonso
Grupo de Espectroscopia Molecular (GEM), Edificio Quifima, Área de Química-Física, Laboratorios de Espectroscopia y Bioespectroscopia, Parque Científico UVa, Unidad Asociada CSIC
Universidad de Valladolid, 47011 Valladolid (Spain)
E-mail: jlalonso@qf.uva.es
Dr. L. Kolesniková
Department of Analytical Chemistry
University of Chemistry and Technology
Technická 5, 16628 Prague 6 (Czech Republic)
Supporting information and the ORCID identification number(s) for the author(s) of this article can be found under: https://doi.org/10.1002/anie.202105718.

© 2021 The Authors. Angewandte Chemie International Edition published by Wiley-VCH GmbH. This is an open access article under the terms of the Creative Commons Attribution Non-Commercial NoDerivs License, which permits use and distribution in any medium, provided the original work is properly cited, the use is non-commercial and no modifications or adaptations are made.

sics need to draw on high-resolution rotational studies, the same wavelengths of the surveys captured by radio telescopes, to detect a molecule in the ISM.[10] Over 200 molecules have already been detected, including important precursors for biomolecular building blocks.[11] The identification of chiral molecules in the interstellar medium is a remarkable fact that could shed light on the origin of the enantiomeric excess. Up to now, propylene oxide is the only chiral molecule observed in the ISM.[12] The identification of any other chiral molecule, i.e., TA, would be a considerable breakthrough.[13]

Owing to its vital importance, the naturally occurring form of TA, the enantiomer (*R*,*R*), has been the subject of several structural studies in condensed phases. The crystal structure was explored using X-ray and neutron diffraction methods, displaying a unique configuration corresponding to a structure with a *trans* (T) disposition of its carbon chain.[14,15] More recently, THz vibrational spectroscopy has been employed, showing a more accurate crystal packaging arrangement of this T configuration.[16] In solution, vibrational circular dichroism (VCD),[17,18] NMR,[19] and vibrational Raman optical activity (ROA)[20,21] show the same T (*trans*) configuration determined in its crystal structure and stabilized by two intramolecular hydrogen bondings between each O–H and C=O group attached to the same chiral carbon. We find it surprising that despite three absolute configurations of the carbon chain are possible, one "*trans*" (T) and two "*gauche*" (G^+, G^-) (see Figure 1), only the "*trans*" form has been observed. Even when diffraction and spectroscopic methods are feasible, their structural description is biased by crystal packing forces and solvent effects, wiping out the conformational variety of TA; they do not reflect its raw structure.

TA contains four hydroxyl groups that can act as proton donors or acceptors, while the two carbonyl groups act as proton acceptors. Even a relatively small molecule, such as TA, is expected to exist in many conformations due to its torsional flexibility based on the seven internal torsions (see Figure 1). From looking at the different torsion angles, we can bring forward different starting configurations shown in Figure 1. The notation used to label each configuration includes the T, G^+, and G^- labels to denote the main carbon chain's configuration, based on the α torsion angle's value. The following two subscripts: s or a, indicate the "*syn*" or "*anti*" arrangement of the hydroxyl group attached to each chiral carbon (C*) concerning its adjacent C=O group of the carboxylic group. Thus, we can anticipate the formation of intricate networks of intramolecular hydrogen bonds that can potentially stabilize many structures and presumably play an important role in the numerous properties developed by this essential molecule. Its conformational analysis requires an experimental study under isolated conditions to disentangle the intramolecular hydrogen bonding puzzle between these adjacent groups. In this context, high-resolution rotational spectroscopy emerges as a unique spectroscopic method that does entirely remove unwanted environmental interference. However, it requires sufficient partial pressure of the analyte in the gas phase. Unfortunately, TA is solid with a high melting point (174 °C) and thermal instability. It cannot be transferred intact into the vapor phase by conventional heating procedures, so unperturbed condition studies have not yet been possible. Despite its essential role, no structural data have been reported for the unbiased tartaric acid. The dicarboxylic succinic acid has been studied by rotational spectroscopy and a *gauche* conformer observed.[22]

A comprehensive structural study of (*R*,*R*) TA has been carried out using rotational spectroscopy coupled to a laser ablation system to fill this structural information gap on this relevant molecule. This strategy allowed us to unveil the natural and dominating conformations that compose TA's structural landscape, avoiding the vaporization issues. This experimental approach has proven ideal for exploring the architecture of numerous solid biomolecules of amino acids,[23] nucleosides,[24] sugars,[25] and dipeptides,[26] among others, constituting a definitive tool in the conformational analysis.

The experiments were performed with the LA-CP-FTMW (laser ablation chirped pulse Fourier transform microwave) spectrometer built at the University of Valladolid.[29,30] The broadband rotational spectrum in the 6–12 GHz frequency range is shown in Figure 2. Previous to its analysis, lines corresponding to known photofragment species and water clusters were identified and removed, and we proceeded to the conformational identification. At first sight, the spectrum is dominated by strong μ_c-type R-branch progressions of $J+1_{1,J} \leftarrow J_{0,J}$, $J+1_{2,J} \leftarrow J_{1,J}$ and $J+1_{2,J-1} \leftarrow J_{1,J-1}$ ($J=1$ to 4) belonging to a dominant species, labeled as rotamer I in Figure 1a. After an iterative process of measuring and fitting[27] rotational transitions, a set of experimental rotational constants for rotamer I was obtained using a semirigid rotor Hamiltonian.[28] They are collected in the first column of Table 1. To ascertain the TA conformer responsible for the intensely observed spectrum of rotamer I, we have to compare the above derived spectroscopic constants with those calculated by ab initio and DFT computational methods (Supporting Information, Tables S6 and S7) complementing previous computational works.[29,30] Table 1 shows the spectroscopic parameters predicted for the six low-energy conformers in an energy window of 1000 cm^{-1} above the global minimum. The comparison allows us to assign the rotamer I unambiguously to the Ts,s conformer. It is predicted as the global minimum and presents a C_2-symmetry with a unique non-zero value of electric dipole moment component in the *c*-axis (see Figure 3) consistent with the observed *c*-type selection rules.

After removing all the lines corresponding to Ts,s conformer, many weaker lines remained unassigned. They should belong to other low-energy conformers of tartaric acid. Following the same procedure, four other rotameric species were assigned, corresponding to G^+a,s, Ta,s (II), G^-a,s, G^-s,s (see Figure 2b and c). All the measured rotational transition frequencies are in the Supporting Information, Tables S1–S5. Finally, different frequency ranges were deeply analyzed to detect the Ta,s (I) conformer, but no lines were found. The absence of spectral signatures attributable to Ta,s(I) conformer could be explained by the low values of dipole moment components (see Table 1). Relative intensity measurements of selected transitions made it possible to evaluate the relative abundance of the observed conformers to be: Tss(~49%), G^+as(~38%), Tas(~7%), G^-aa(~5%), G^-ss(~1%). Scale

 © 2021 The Authors. Angewandte Chemie International Edition published by Wiley-VCH GmbH

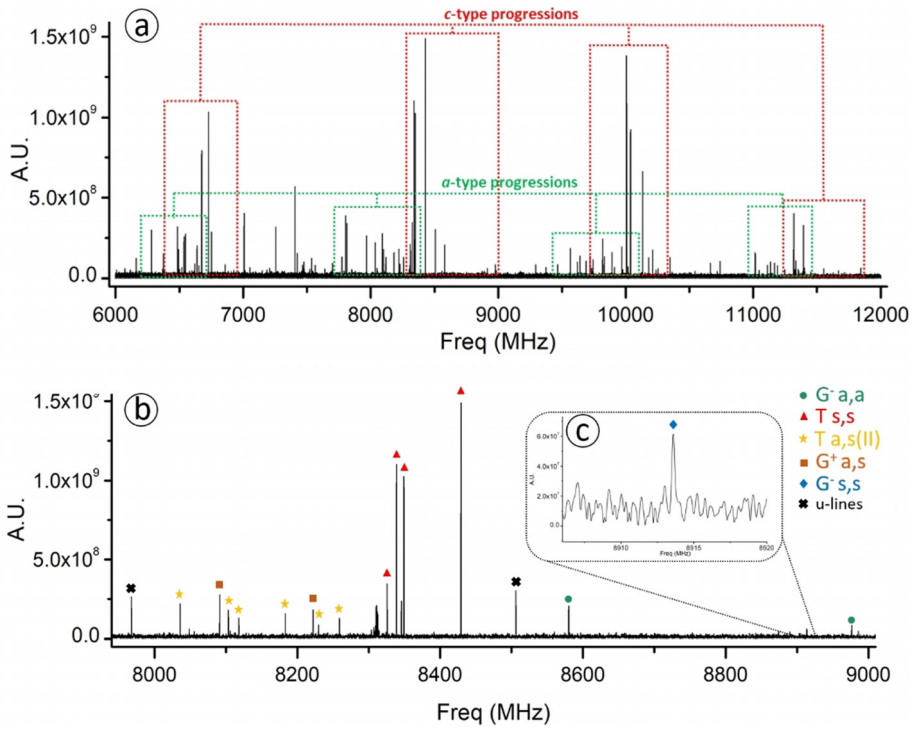

Figure 2. a) Broadband rotational spectrum of (*R*,*R*) Tartaric acid from 6 to 12 GHz. The spectrum is dominated by strong (and also weaker) μ_c R-branch rotational transitions progressions for T,s,s, T,a,s(II), G^-,a,a and G^-,s,s and weaker μ_a R-branch rotational transitions progressions for G^+,a,s and T,a,s (II). b) A spectrum fragment showing identified transitions of the observed conformers. c) A ×20 superzoom showing a weak transition of the G^-,s,s conformer.

factors ranging from 0.996 to 1.014 bring the MP2 ab initio values of the rotational constants into coincidence with the experimental ones, reflecting the excellent match between theory and experiment. Consequently, the ab initio structures can be taken as a good approximation of the actual structures for the five TA conformers. The estimated relative abundances on the other hand, show small variations with those predicted using the calculated energies. This fact shows the importance of microwave data as a benchmark to improve and develop accurate computational chemistry methods.

The structures of the five detected conformers of TA, depicted in Figure 3, can be rationalized in terms of the intramolecular hydrogen bonding networks responsible for their stabilization. The most abundant Ts,s conformer appears over stabilized by two O–H···O=C hydrogen bonds between the OH group of each asymmetric carbon (C*) and its vicinal O=C of the carboxylic group reinforced by two terminal *cis*-carboxylic interactions keeping a C_2-symmetry. Four cooperative intramolecular hydrogen bonds, two O–H···O–H type and another two O–H···O=C type, are responsible for stabilizing the three G^+a,s, G^-a,a, and G^-s,s *gauche* conformers. Conformer G^+a,s stabilizes its structure through a cooperative OH···O-H···OH···O=C network extended along the carbon chain and closing a seven-membered cyclic network through an O–H···O=C between the two terminals carboxylic groups in a *trans*-arrangement. The other C_2 symmetry conformers G^-a,a and G^-s,s stabilizes its structure through two cooperative OH···OH···O=C hydrogen-bond networks forming two six-membered cyclic networks for each of them. The formation of six or seven-membered cyclic networks contributes to the

Table 1: Experimental spectroscopic parameters for the five observed rotamers of tartaric acid.

	T,s,s Rotamer I[e]	Theor.[f]	T,a,s (I) Theor.	G^+,a,s Rotamer II	Theor.	T,a,s (II) Rotamer III	Theor.	G^-,a,a Rotamer IV	Theor.	G^-,s,s Rotamer V	Theor.
A[a]	2501.57910(86)[g]	2490	2505	2086.53041(96)	2082	2477.6433(23)	2488	1823.17494(81)	1823	1781.89105(74)	1772
B	844.52864(48)	849	843	1078.70088(40)	1080	825.84623(72)	824	1169.0241(10)	1167	1189.31507(75)	1199
C	833.92841(53)	845	819	748.80543(41)	754	796.37217(86)	803	980.81467(94)	995	971.8262(13)	982
D_J	0.0441(78)			0.0311(61)		0.0435(83)		0.168(29)		0.197(13)	
D_{JK}	0.249(28)			0.197(38)		–		–		0.196(40)	
μ_a	–	0.0	−0.8	obs.	−1.6	obs.	−3.7	–	0.0	–	0.0
μ_b	–	0.0	−0.2	obs.	2.6	–	−0.4	–	0.0	–	0.0
μ_c	obs.	−2.5	0.0	–	0.0	obs.	−1.8	obs.	2.6	obs.	3.7
N[b]	29	–		51		24		16		15	
σ [c]	6.0	–		7.7		8.9		6.6		2.5	
ΔE_{ZPE}	–	0	556		762		960		906		873
ΔG[d]	–	0	697		1203		1169		1301		1345

[a] A, B, and C represent the rotational constants (in MHz); D_J, D_{JK} represent the determined centrifugal distortion constants (in kHz); μ_a, μ_b, and μ_c are the electric dipole moment components (in D). [b] Number of fitted transitions. [c] RMS deviation of the fit in kHz. [d] Relative energies (in cm^{-1}) with respect to the global minimum, taking into account the zero-point energy (ZPE). Gibbs energies (in cm^{-1}) calculated at 298 K. [e] Experimentally determined rotational and centrifugal constants. [f] Theoretically predicted rotational constants at the MP2 level. [g] Standard error in parentheses in the last digit units.

 © 2021 The Authors. Angewandte Chemie International Edition published by Wiley-VCH GmbH

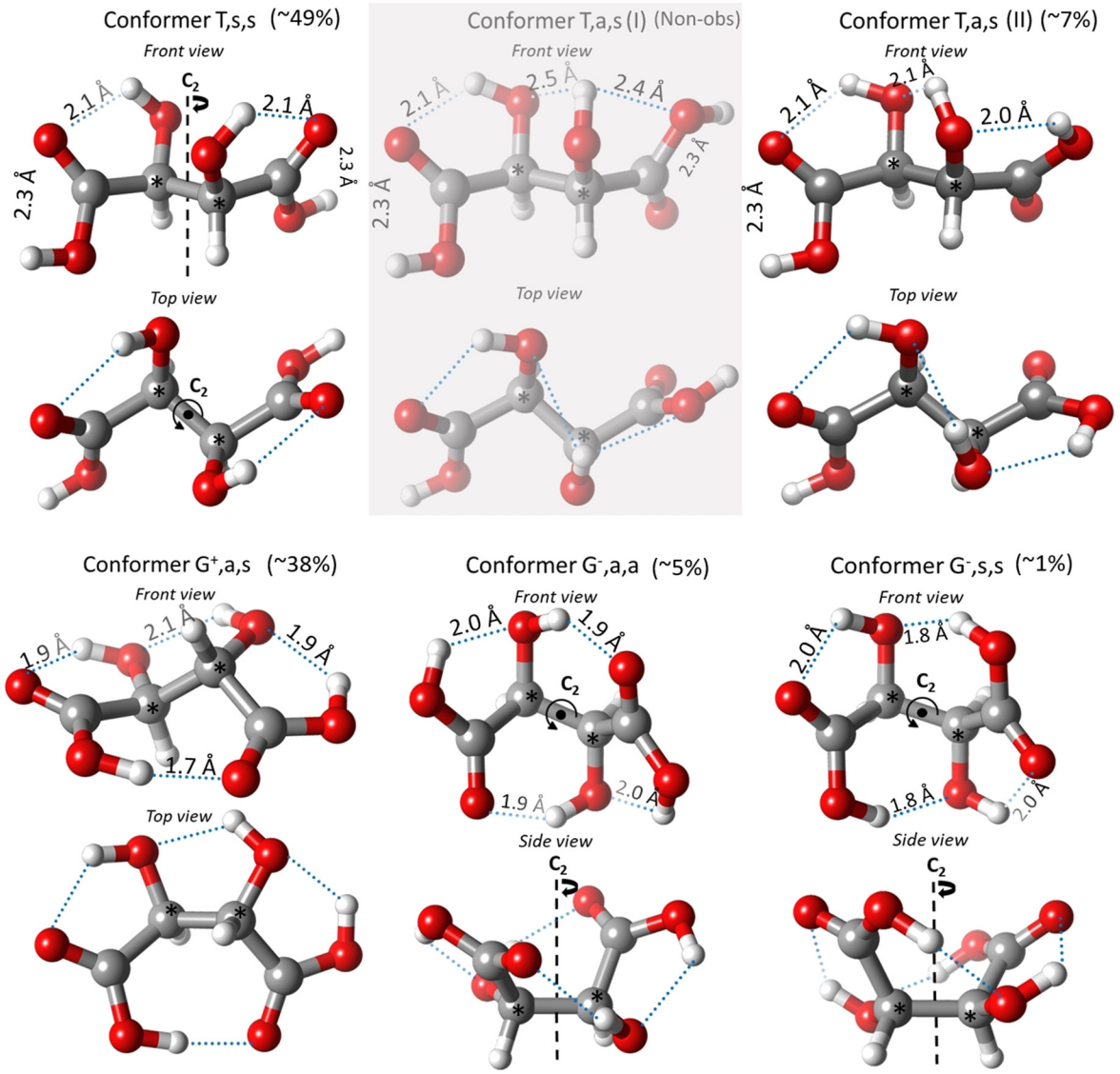

Figure 3. Close-up picture of the *trans* and *gauche* tridimensional structures of the five observed conformers and non-observed Ta,s(I) conformer of tartaric acid showing the intramolecular hydrogen bonding networks (distances) that stabilize them calculated at MP2 6–311++G(d,p) level.

over-stabilization of the *gauche* conformers compared to the less abundant Ta,s(II) conformer. Three cooperatives OH···OH···OH···O=C hydrogen bonds extended along the carbon chain, stabilize this last observed conformer. With the hydrogen bonding interactions verified by the NCIPLOT program,[31–33] where the reduced gradient of the electronic density is 3D represented, there is a more detailed view of the places involved in the intramolecular interactions (Supporting Information, Figure S1).

As mentioned above, TA is found only in the *trans* configuration in condensed phases, both in the crystal and solution.[14–19] Strikingly, TA's isolated structures observed in the supersonic expansion of our experiment comprise both *trans* and *gauche* forms almost equally populated. This remarkable fact should be explained by looking at the structure and interactions that may take place in the different conformers. In the *trans*-TA structures (see Figures 3 and S1), the carboxylic groups are not involved in any intramolecular interaction. The opposite is true for the *gauche*-TA forms; both acidic groups participate in intramolecular hydrogen bonding networks. These observations may indicate that the *trans-TA* configuration allows the monomers to interact with each other at both ends through a double O–H···O=C interaction, allowing a natural extension of the TA units forming a kind of TA intermolecular chain. Additionally, the *trans* configuration allows the interaction between the chain's central hydroxyl groups in a parallel disposition, resulting in strong hydrogen bonds between the TA chains. All this reinforces the existence of the *trans* forms in condensed phases, which is not possible in the *gauche* arrangement.

In conclusion, the discriminating power obtained combining the high-quality rotational data provided by our LA-CP-FTMW technique with those of high-level quantum chemical calculations has enabled disentangling the conformational puzzle of TA. Five naked structures of TA have been unequivocally identified, leading to the first determination

 © 2021 The Authors. Angewandte Chemie International Edition published by Wiley-VCH GmbH

of its conformational landscape. It is precious information since the behavior in solution should fluctuate between the most stable *trans* structures found in the isolation conditions of the gas phase.

The study provides direct and comprehensive information, at the atomic resolution, on the hydrogen bond networks of tartaric acid that exist as a result of O–H···O–H, and O–H···O=C contacts, closing five-, six-, or seven-membered cyclic structures. The detected conformers adapt their molecular shapes to optimize the sequence of intramolecular hydrogen bonds, increasing their strength by cooperativity.[34,35]

Last but not least, the experimental set of rotational parameters enable, for the first time, the search of TA in the interstellar medium. Except for propylene oxide, all the complex organic molecules detected in the interstellar medium are achiral. The detection of another chiral molecule is one of the most pursued targets in astrobiology to try to shed light on the quest of chirality in the interstellar medium and the origin of life. In the event that its detection is not possible in the actual surveys from radiotelescopes, with the advances that continuously happen in radioastronomy, this data will still be essential for possible future identifications. Present results show the vital role of chemistry laboratory experiments in the astrophysics field.

Acknowledgements

The financial fundings from Ministerio de Ciencia e Innovación (CTQ2016- 76393-P and PID2019-111396GB-I00) and Junta de Castilla y León (Grants VA077U16 and VA244P20) are gratefully acknowledged. E.R.A. thanks Ministerio de Ciencia e Innovación for a Juan de la Cierva de formación grant (FJC2018-037320-I).

Conflict of Interest

The authors declare no conflict of interest.

Keywords: astrochemistry · chiral molecules · laser ablation · rotational spectroscopy · tartaric acid

[1] L. Pasteur, *Ann. Chim. Phys.* **1848**, *24*, 442 – 459.
[2] J.-B. Biot, *Mem. Acad. Sci. Inst. Fr.* **1817**, *2*, 4 – 136.
[3] H. D. Flack, *Acta Crystallogr. Sect. A* **2009**, *65*, 371 – 389.
[4] J. Gal, *Helv. Chim. Acta* **2013**, *96*, 1617 – 1657.
[5] "Tartaric Acid—Chemical Economics Handbook (CEH) | IHS Markit", can be found under https://ihsmarkit.com/products/tartaric-acid-chemical-economics-handbook.html.
[6] J. Gawronski, K. Gawronska, *Tartaric & Malic Acids in Synthesis: A Source Book of Building Blocks, Ligands, Auxiliaries & Resolving Agents*, Wiley, Hoboken, **1999**.
[7] D. Seebach, A. K. Beck, A. Heckel, *Angew. Chem. Int. Ed.* **2001**, *40*, 92 – 138; *Angew. Chem.* **2001**, *113*, 96 – 142.
[8] K. Gratzer, G. N. Gururaja, M. Waser, *Eur. J. Org. Chem.* **2013**, 4471 – 4482.
[9] G. Cooper, N. Kimmich, W. Belisle, J. Sarinana, K. Brabham, L. Garrel, *Nature* **2001**, *414*, 879 – 883.
[10] E. Herbst, E. F. van Dishoeck, *Annu. Rev. Astron. Astrophys.* **2009**, *47*, 427 – 480.
[11] B. A. McGuire, *ApJS* **2018**, *239*, 17.
[12] B. A. McGuire, P. Brandon Carroll, R. A. Loomis, I. A. Finneran, P. R. Jewell, A. J. Remijan, G. A. Blake, *Science* **2016**, *352*, 1449 – 1452.
[13] Y. Ellinger, F. Pauzat, A. Markovits, A. Allaire, J.-C. Guillemin, *Astron. Astrophys.* **2020**, *633*, A49.
[14] F. Stern, C. A. Beevers, *Acta Crystallogr.* **1950**, *3*, 341 – 346.
[15] Y. Okaya, N. R. Stemple, M. I. Kay, *Acta Crystallogr.* **1966**, *21*, 237 – 243.
[16] E. M. Witko, T. M. Korter, *J. Phys. Chem. A* **2011**, *115*, 10052 – 10058.
[17] P. L. Polavarapu, C. S. Ewig, T. Chandramouly, *J. Am. Chem. Soc.* **1987**, *109*, 7382 – 7386.
[18] J. Gawroński, K. Gawrońska, P. Skowronek, U. Rychlewska, B. Warzajtis, J. Rychlewski, M. Hoffmann, A. Szarecka, *Tetrahedron* **1997**, *53*, 6113 – 6144.
[19] J. Ascenso, V. M. S. Gil, *Can. J. Chem.* **1980**, *58*, 1376 – 1379.
[20] L. D. Barron, A. R. Gargaro, L. Hecht, P. L. Polavarapu, H. Sugeta, *Spectrochim. Acta Part A* **1992**, *48*, 1051 – 1066.
[21] L. D. Barron, *Tetrahedron* **1978**, *34*, 607 – 610.
[22] M. K. Jahn, E. Méndez, K. P. Rajappan Nair, P. D. Godfrey, D. McNaughton, P. Écija, F. J. Basterretxea, E. J. Cocinero, J. U. Grabow, *Phys. Chem. Chem. Phys.* **2015**, *17*, 19726 – 19734.
[23] I. León, E. R. Alonso, S. Mata, C. Cabezas, J. L. Alonso, *Angew. Chem. Int. Ed.* **2019**, *58*, 16002 – 16007; *Angew. Chem.* **2019**, *131*, 16148 – 16153.
[24] I. Peña, C. Cabezas, J. L. Alonso, *Angew. Chem. Int. Ed.* **2015**, *54*, 2991 – 2994; *Angew. Chem.* **2015**, *127*, 3034 – 3037.
[25] E. R. Alonso, I. Peña, C. Cabezas, J. L. Alonso, *J. Phys. Chem. Lett.* **2016**, *7*, 845 – 850.
[26] I. León, E. R. Alonso, C. Cabezas, S. Mata, J. L. Alonso, *Commun. Chem.* **2019**, *2*, 3.
[27] H. M. Pickett, *J. Mol. Spectrosc.* **1991**, *148*, 371 – 377.
[28] W. Gordy, R. L. Cook, *Microwave Molecular Spectra*, Wiley, Hoboken, **1984**.
[29] M. Hoffmann, A. Szarecka, J. Rychlewski, *Adv. Quantum Chem.* **1998**, *32*, 109 – 125.
[30] M. Hoffmann, J. Rychlewski, U. Rychlewska, *Comput. Methods Sci. Technol.* **1996**, *2*, 51 – 63.
[31] E. R. Johnson, S. Keinan, P. Mori-Sánchez, J. Contreras-García, A. J. Cohen, W. Yang, *J. Am. Chem. Soc.* **2010**, *132*, 6498 – 6506.
[32] J. Contreras-García, E. R. Johnson, S. Keinan, R. Chaudret, J. P. Piquemal, D. N. Beratan, W. Yang, *J. Chem. Theory Comput.* **2011**, *7*, 625 – 632.
[33] R. A. Boto, F. Peccati, R. Laplaza, C. Quan, A. Carbone, J. P. Piquemal, Y. Maday, J. Contreras-García, *J. Chem. Theory Comput.* **2020**, *16*, 4150 – 4158.
[34] G. A. Jeffrey, *An Introduction to Hydrogen Bonding*, Oxford University Press, Oxford, **1997**.
[35] M. López de la Paz, G. Ellis, M. Pérez, J. Perkins, J. Jiménez-Barbero, C. Vicent, *Eur. J. Org. Chem.* **2002**, 840 – 855.

Manuscript received: April 27, 2021
Accepted manuscript online: June 1, 2021
Version of record online: July 1, 2021

 © 2021 The Authors. Angewandte Chemie International Edition published by Wiley-VCH GmbH